Hygroscopic growth of atmospheric and model humic-like substances

E. Dinar,[1] I. Taraniuk,[1] E. R. Graber,[2] T. Anttila,[3,4] T. F. Mentel,[3] and Y. Rudich[1]

Received 26 April 2006; revised 5 October 2006; accepted 18 October 2006; published 13 March 2007.

[1] The hygroscopic growth (HG) of humic-like substances (HULIS) extracted from smoke and pollution aerosol particles and of Suwannee River fulvic acid (SRFA, bulk and fractions of different molecular weight) was measured by humidity tandem differential mobility analyzer (H-TDMA). By characterizing physical and chemical parameters such as molecular weight, elemental composition, and surface tension, we test the effect of these parameters on particle interactions with water vapor. For molecular weight-fractionated SRFA fractions, the growth factor at 90% relative humidity was generally inversely proportional to the molecular weight. HULIS extracts from ambient particles are more hygroscopic than all the SRFA fractions and exhibit different hygroscopic properties depending on their origin and residence time in the atmosphere. The results point out some dissimilarities between SRFA and aerosol-derived HULIS. The cloud condensation nuclei (CCN) behavior of the studied materials was predicted on the basis of hygroscopic growth using a recently introduced approach of Kreidenweis et al. (2005) and compared to CCN activity measurements on the same samples (Dinar et al., 2006). It is found that the computational approach (Kreidenweis et al., 2005) works reasonably well for SRFA fractions but is limited in use for the HULIS extracts from aerosol particles. The difficulties arise from uncertainties associated with HG measurements at high relative humidity, which leads to large errors in the predicted CCN activity.

Citation: Dinar, E., I. Taraniuk, E. R. Graber, T. Anttila, T. F. Mentel, and Y. Rudich (2007), Hygroscopic growth of atmospheric and model humic-like substances, *J. Geophys. Res.*, *112*, D05211, doi:10.1029/2006JD007442.

1. Introduction

[2] Many climate-related phenomena are directly and indirectly affected by atmospheric aerosols [*Andreae et al.*, 2005; *Hansen et al.*, 2005; *Intergovernmental Panel on Climate Change*, 1995, 2001; *Kaufman et al.*, 2005; *Koren et al.*, 2005; *Novakov and Corrigan*, 1996; *Ramanathan et al.*, 2001]. At supersaturation conditions (SS, RH > 100%), activation of aerosol particles to cloud droplets can modify cloud growth, reflectance, and lifetime [*Kaufman et al.*, 2005; *Koren et al.*, 2005; *Ramanathan et al.*, 2001; *Rosenfeld*, 2000]. Under subsaturation (SubS) conditions (RH $\leq$ 100%), the hygroscopic growth (HG) of aerosol particles determines their water content and hence aerodynamic size, optical properties and ability to participate in heterogeneous chemical processes. As a result, hygroscopic growth affects visibility and aerosol lifetime, as well as particle deposition in the lung and in the upper respiratory airways [*Bragatto et al.*, 2002; *Menache et al.*, 1996; *Ramachandran et al.*, 1996; *Virtanen et al.*, 2004]. Hence it is clear that aerosol hygroscopic properties exert an important control over the diverse effects of aerosol particles on atmospheric processes [*Raes et al.*, 2000]. Considering this, the ability to predict aerosol hygroscopic growth and CCN activity on the basis of their chemical nature would be a welcome advance. Recent studies have suggested that knowledge of the subsaturation hygroscopic properties of aerosol particles can be used to predict their behavior at supersaturation conditions [*Koehler et al.*, 2006; *Kreidenweis et al.*, 2005].

[3] A significant fraction of the organic component in atmospheric aerosol particles consists of water-soluble multifunctional organic compounds [*Decesari et al.*, 2000; *Facchini et al.*, 1999b; *Kiss et al.*, 2002; *Krivacsy et al.*, 2001; *Saxena and Hildemann*, 1996; *Varga et al.*, 2001; *Zappoli et al.*, 1999] which bear a certain resemblance to humic substances (HS) common in soils and aqueous environments [*Graber and Rudich*, 2006]. Humic-like substances, or HULIS, have been identified in rural and urban aerosol particles [*Cini et al.*, 1996; *Decesari et al.*, 2001; *Facchini et al.*, 2000, 1999a; *Havers et al.*, 1998; *Samburova et al.*, 2005; *Zappoli et al.*, 1999], in fog water [*Cappiello et al.*, 2003; *Facchini et al.*, 2000; *Herckes et al.*, 2002; *Krivacsy et al.*, 2000], in marine particulate samples [*Simoneit*, 1980], and in biomass-burning aerosols [*Mayol-Bracero et al.*, 2002]. HULIS consist of polydisperse,

[1]Department of Environmental Sciences, Weizmann Institute of Science, Rehovot, Israel.
[2]Institute of Soil, Water, and Environmental Sciences, Volcani Center, Bet Dagan, Israel.
[3]Institute for Tropospheric Chemistry, Research Center Jülich, Jülich, Germany.
[4]Now at Research and Development, Finnish Meteorological Institute, Helsinki, Finland.

0148-0227/07/2006JD007442

polyfunctional compounds made up of a heterogeneous mixture of aliphatic and aromatic structures with substituted acidic, phenolic, and ester functional groups [*Decesari et al.*, 2001; *Graber and Rudich*, 2006; *Gysel et al.*, 2004; *Kiss et al.*, 2002; *Krivacsy et al.*, 2001; *Mayol-Bracero et al.*, 2002; *Varga et al.*, 2001].

[4] Since HULIS are commonly found in atmospheric aerosol particles in many locations, making up between 15–60% of aerosol particle mass (in the tropics and midlatitudes), there is a need to better understand their contribution to aerosol physical and chemical properties. In spite of its importance, most studies concerning HULIS hygroscopic growth under subsaturation conditions have employed model compounds, mainly terrestrial and aquatic humic and fulvic acids [*Brooks et al.*, 2004; *Chan and Chan*, 2003; *Gysel et al.*, 2004; *Svenningsson et al.*, 2006]. As far as we know, the hygroscopic properties of authentic HULIS under SubS conditions have been examined only by *Gysel et al.* [2004]. Considering the abundance of HULIS in aerosol, there is still a fundamental need to characterize how the hygroscopic growth of aerosols containing HULIS depends on molecular parameters such as molecular weight, chemical composition and surface tension of the HULIS, and whether the model compounds which are often used indeed provide a good proxy for atmospheric HULIS. There is also a need to compare hygroscopic behavior of HULIS obtained from different types of sources, and having undergone varying extents of atmospheric processing.

[5] In a recent study, we compared measured activation diameters of HULIS isolated from the water soluble extract of airborne fresh and aged wood-burning particles and from urban pollution particles, to those of fulvic acid (FA) from an aquatic source (Suwannee River fulvic acid, SRFA) [*Dinar et al.*, 2006]. The experimental results indicated that atmospheric HULIS readily activate to cloud droplets and that the Köhler theory efficiently predicts their activation diameters, provided that the molecular weight and surface tension of the HULIS are known or well-estimated. To complement that study, we herein investigate the hygroscopic growth of the same HULIS samples under subsaturation conditions, with specific aims: (1) to examine and compare hydration behavior of atmospheric HULIS from different sources with that of molecular weight-fractionated standard aquatic FA; (2) to relate hygroscopic growth to various chemical and physical characteristics; and (3) to test whether CCN activity of HULIS can be predicted from subsaturation behavior.

2. Experimental Procedure

2.1. General Procedure

[6] All the experiments under SubS conditions were conducted using a Humidified Tandem Differential Mobility Analyzer (H-TDMA) setup. A detailed description of the molecular weight separation methodology and HULIS sampling and isolation are given by *Dinar et al.* [2006]. Therefore only a brief description is given here.

2.1.1. Aerosol Sampling and HULIS Extraction

[7] Three samples of atmospheric particles were collected: (1) fresh smoke particles sampled during the night of a nationwide intensive wood-burning event (a holiday called "Lag B'Omer", 26–27 May 2005), with an average PM10 mass concentration near the sampling site of 300–400 $\mu g\ m^{-3}$ of smoke, (2) slightly aged wood-burning smoke particles sampled during the day following the fires (27 May 2005), with PM10 mass concentrations of 60–180 $\mu g\ m^{-3}$, and (3) photochemical pollution particles sampled only during daytime for a three week period (26 July to 16 August 2005), with average PM10 mass concentration of about 25 $\mu g\ m^{-3}$. The atmospheric conditions during the 3 weeks period were relatively constant. The three samples will be termed in this paper LBO-night (fresh smoke), LBO-day (slightly aged smoke) and 3WSFA (3 weeks sampling of urban pollution particles). Aerosol loadings were measured by the Israel Ministry of Environment.

[8] Water soluble fulvic acid type HULIS (FA-HULIS) were extracted from the filters and separated from other components by an extraction and isolation procedure developed on the basis of the scheme recommended by the International Humic Substances Society (IHSS) for aquatic fulvic acids, and adapted by us for airborne particulate matter collected on quartz fiber filters. The samples were characterized to obtain estimated number averaged molecular weight (M_N), aromaticity and surface tension [*Dinar et al.*, 2006]. The number average molecular weight is the common average of the molecular weights of the individual macromolecules. A detailed description of the sampling procedure and HULIS extraction and characterization is given by *Dinar et al.* [2006].

2.1.2. Suwannee River Fulvic Acid Samples

[9] Suwannee River fulvic acid (SRFA) of reference grade obtained from the IHSS (product number 1R101F) was used as the laboratory model for atmospheric HULIS. SRFA was used in several previous laboratory studies as a representative for atmospheric HULIS [*Abdul-Razzak and Ghan*, 2004; *Brooks et al.*, 2004; *Chan and Chan*, 2003; *Fuzzi et al.*, 2001; *Haiber et al.*, 2001; *Kiss et al.*, 2005; *Mircea et al.*, 2002; *Nenes et al.*, 2002; *Samburova et al.*, 2005; *Svenningsson et al.*, 2006]. Because the average molecular weight of atmospheric HULIS was reported to be smaller on average than that of fulvic acids (number weight average of about 450 Da) [*Graber and Rudich*, 2006; *Kiss et al.*, 2003; *Rostad and Leenheer*, 2004], the SRFA was separated into different molecular weight fractions by ultrafiltration.

[10] The goal of the separation was to obtain a set of model compounds with different molecular weights that may be more similar in character and behavior to HULIS and to investigate if and how properties systematically change with average molecular weight. We developed an ultrafiltration protocol that provides five fractions of water-soluble material with different average molecular weight. The nominal molecular weight ranges of the filters used are: 0.2–0.5 kDa, 0.5–1.0 kDa, 1–3 kDa, 3–10 kDa, and 10–30 kDa. The obtained fractions are termed F1, F2, F3, F4, and F5, respectively; they were characterized for the number averaged molecular weight (M_N), percent aromaticity, and surface tension. Elemental composition and acidity measurements were also conducted.

2.2. Atomized Solutions

[11] All investigated samples were prepared as dilute aqueous solutions using 18.2 MOhm Mill-Q water: 20–50 mg/L for ammonium sulfate (AS) and SRFA samples and 10–20 mg/L for atmospheric HULIS samples. The

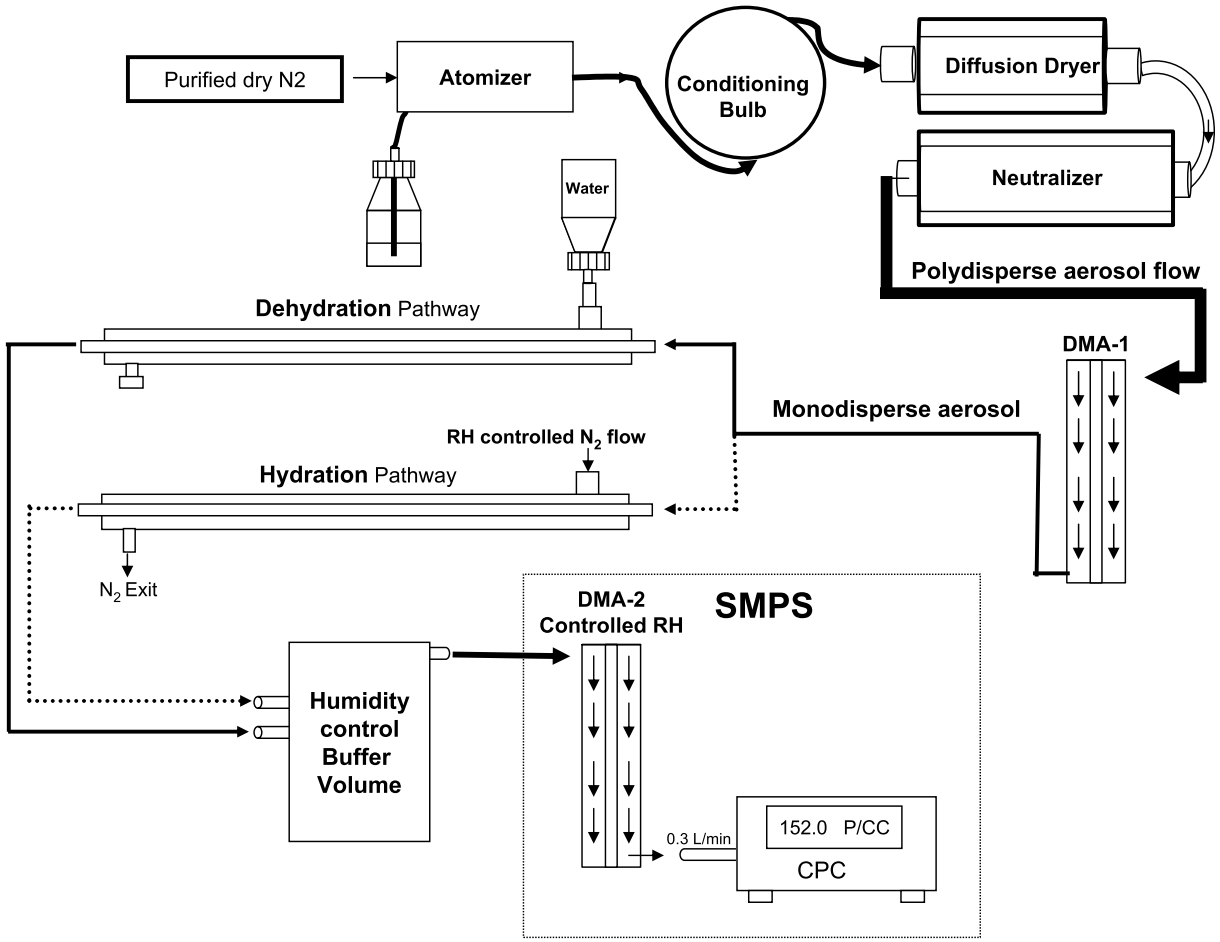

Figure 1. Illustration of the humidity tandem differential mobility analyzer (H-TDMA) setup used in this work. After particles have been conditioned, dried, charged, and size selected (by Differential Mobility Analyzer, DMA-1), they can be directed toward the hydration pathway (dashed line, dry Nafion) or alternatively to the dehydration pathway (solid line, wet Nafion) after they have been exposed to 100% relative humidity (RH). As particles exit the Nafion, they enter the RH-controlled buffer volume. The last stage of adaptation to the final RH occurs in the RH-controlled Scanning Mobility Particle Sizer (SMPS), where particles are measured for their RH-dependent mean diameter.

solutions were atomized using a TSI constant output atomizer (TSI-3076) operating at 20 PSI ($\sim$2 standard liters per minute (SLM)) with particle-free pure nitrogen, generating a polydisperse distribution of droplets (mean diameter $\sim 0.3\mu$m).

2.3. Chemical and Physical Characterization

[12] Number average molecular weights of the different samples were estimated using correlations between UV absorbance and molecular weight and aromaticity of different aquatic and terrestrial fulvic acids samples available in the literature [*Chin et al.*, 1994; *Schafer et al.*, 2002]. Surface tension was measured using the pendent drop method [*Eastoe and Dalton*, 2000]. Acidity was measured by titration with KOH. All samples were H^+-saturated and free of salts and small organic acids, as verified by ion chromatography. Detailed description of these measurements and the estimation methods is given by *Dinar et al.* [2006].

2.4. Hygroscopic Growth Experiments

[13] The hygroscopic growth factor (GF) is the relative size increase of particles due to water uptake. It is defined as: $GF_{RH} = \frac{D_{RH}}{D_0}$, where D_0 is the particle dry diameter, and D_{RH} is its diameter at a specific RH.

[14] A schematic illustration of the experimental setup is shown in Figure 1. The flow from the atomizer entered a 10 L conditioning bulb with a residence time of about 16 minutes before entering diffusion dryers (RH < 3%). The "conditioning" step allows the particle to reach optimal structure upon drying, ensuring a constant electromobility diameter and formation of spherical aerosols [*Kramer et al.*, 2000; *Mikhailov et al.*, 2004; *Weingartner et al.*, 1995]. The dry polydisperse aerosol was neutralized, and directed into a Differential Mobility Analyzer (DMA-1) operating with a dry (RH < 3%) clean sheath flow. The resulting size-selected monodisperse flow (60 nm for all experiments and a constant number concentration for all experiments) passed through a Nafion tube in which humidity was controlled.

[15] Growth factors were measured for particles undergoing both hydration (i.e., increasing RH) and dehydration (decreasing RH) to test for hysteresis. For the hydration and dehydration experiments, measurements started by directing

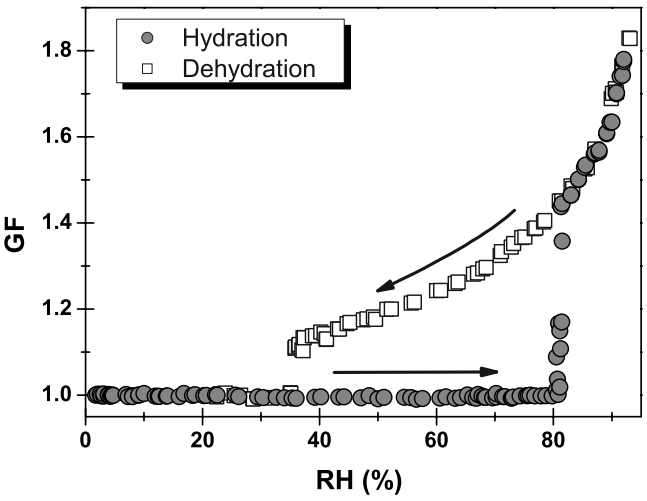

Figure 2. Hygroscopic growth of ammonium sulfate particles. The open squares indicate the dehydration process (evaporation), with efflorescence occurring at RH = 36.5%. The gray circles show the hydration process with a deliquescence point at RH = 80.4%. The GF_{90} = 1.7.

a dry monodisperse aerosol flow into a Nafion humidifier, in which RH up to 95% could be reached. The wet particles entered a 1 liter buffer volume (at the same RH), allowing them to reach equilibrium (45–90 s) thus avoiding mass transfer issues [*Chan and Chan*, 2005]. The resulting size change was measured in a humidity-matched Scanning Mobility Particle Sizer (SMPS, DMA-2, and condensation particle counter). SubS hydration growth curves were obtained by measuring particle diameters as a function of increasing RH.

[16] In dehydration experiments, the monodisperse dry particles were exposed to ~100% RH before being exposed to a lower RH. The size change was measured by the RH-controlled SMPS. The lower RH was controlled using an injector-adjusted silica gel diffusion dryer in conjugation with a diluting dry nitrogen flow (not shown in the illustration). In both hydration and dehydration experiments, the SMPS DMA sheath flow RH was controlled. The RH was constantly monitored online (with RH monitors and dew point hygrometer) in several places: (1) following DMA-1, (2) before the SMPS, and (3) in the SMPS sheath flow. During all experiments, the temperature was 22 ± 1°C. Comparative RH measurements between the incoming sample and the humidified DMA over the entire RH range were within <1%. For each sample, growth factor was measured in 0.3–3% RH intervals from ~3% to ~95% RH. An empirical exponential linear fit (y = p1*exp(−x/p2) + p3 + p4*x) was applied to the growth factor versus relative humidity curves. This fit has a very high correlation coefficient (Table 2).

[17] The initially narrow size distributions of particles around an average diameter of 60 nm were not symmetric, with a steeper increase at smaller diameters and a longer tail toward larger diameters. The average mean dry diameter, D_0, was measured at the beginning and end of each run. For all growth factor measurements, the experimental standard deviation did not exceed ±0.008, which corresponds to a change in the monodisperse spectra mean diameter of ~±0.5 nm (for GF_{90} = ~1.23).

3. Results and Discussion

3.1. System Validation Using Ammonium Sulfate Particles

[18] The hygroscopic growth setup was validated by comparing the phase transitions and GF of ammonium sulfate (AS) as a function of RH, to literature values. Figure 2 shows hydration and dehydration curves of 60 nm well-conditioned AS particles. Deliquescence occurred at RH = 80.4 ± 0.3% (Figure 2, gray circles, from left to right). Efflorescence occurred at RH = 36.5 ± 0.5% (Figure 2, open squares, from right to left) and the GF at RH = 90% (GF_{90}) was 1.7 ± 0.008. These results are in very good agreement with earlier studies (*Cruz and Pandis* [2000] measured deliquescence RH (DRH) at 79 ± 1%, *Cziczo and Abbatt* [1999] measured DRH and efflorescence RH at 79 ± 1% and 33.2 ± 2%, respectively, and *Gysel et al.* [2002] measured DRH and GF_{90} to be 80 ± 1.2% and 1.69, respectively).

3.2. Chemical and Physical Characterization of the Samples

3.2.1. Molecular Weight Estimate, Aromaticity, and Elemental Composition

[19] Correlations of UV absorption and molecular weight were used previously for SRFA and atmospheric HULIS by *Dinar et al.* [2006]. The number averaged molecular weight (M_N) of the SRFA fractions, estimated by the correlation provided by *Schafer et al.* [2002], increased from 440 Da to 740 Da from F1–F5 with the bulk SRFA giving 570 Da. The average M_N of the HULIS-FA aerosol extracts are 610, 410 and 500 Da for the LBO-night, LBO-day and 3WSFA samples, respectively. For SRFA, aromaticity increased with increasing molecular weight, and with it, the brown color of the sample. Physical and chemical properties are summarized in Table 1. (For more information on molecular weight and aromaticity determination and on elemental analysis composition of SRFA, see the work of *Dinar et al.* [2006]).

3.2.2. Surface Tension

[20] Surface tension of 1 g L^{-1} aqueous solutions of the SRFA fractions and the HULIS extracts after 90 min (ST_{90}) equilibration is given in Table 1. The most surface active of the SRFA fractions is F1 (M_N of 440 Da), with a ST_{90} of 57 dyn/cm. ST_{90} of the other fractions varied from ~63 for F2 (average M_N of 520 Da), to 60 for both F3 and F5 (average M_N of 620 and 740 Da, respectively). There was no clear relationship between ST_{90} and the estimated molecular weight. The HULIS samples were substantially more surface active than the F1 and F2 SRFA fractions, with ST_{90} values for HULIS extracted from fresh and aged smoke particles of 45 and 44 dyn/cm (LBO-night and LBO-day, respectively), and 56 dyn/cm for the 3 week photochemical pollution samples (3WSFA). Greater surface activity for HULIS extracted from rural aerosols as compared with aquatic fulvic acids has been previously reported also by *Kiss et al.* [2005].

3.2.3. SRFA Acidity

[21] The results of the titrations of SRFA are given in Table 1. The acidity content per carbon generally decreases

Table 1. Estimated Chemical and Physical Parameters of the Different Samples, Including Number-Averaged Molecular Weight (M_N), Aromaticity, Surface Tension (ST_{90}), and Acidity[a]

Sample	M_N	Aromaticity,%	ST_{90} at 90 Minutes, 1g/L, dyn/cm	Titration Until pH = 8 mmol Acidic Groups g^{-1}	Titration Until pH = 8 mmol Acidic Groups/g OC	O/C Mole Ratio
F1	440	12	57.1 ± 0.9	4.4	8.0	0.54
F2	520	16	62.8 ± 0.3	5.6	11.0	0.64
F3	620	23	59.5 ± 0.4	5.0	9.9	0.65
F4	720	30	62.1 ± 0.4	4.4	8.4	0.61
F5	740	32	59.5 ± 1.2	3.8	7.6	0.68
SRFA bulk	570	20	59.0 ± 0.7	5.1	9.6	0.57
LBO-night	610	20	45.4 ± 3.3	-	-	-
LBO-day	410	10	43.9 ± 1.6	-	-	-
3WSFA	500	16	55.5 ± 0.4	-	-	-

[a]M_N was estimated on the basis of correlations given by *Schafer et al.* [2002]. Aromaticity was estimated on the basis of correlations of *Peuravuori and Pihlaja* [1997]. Owing to the small quantities, the acidity of the extracted humic-like substances (HULIS) could not be measured.

with increase of molecular weight with the exception of the F1 fraction. The titration curves indicate that SRFA is a weak acid, and at atmospherically relevant concentrations, such as 1 g/L [*Kiss et al.*, 2005], the dissociation in aqueous solution can be calculated to be approximately 20%. The average number of carboxylic groups per molecule in each fraction range between ~2 for F1 to ~3 for F5, and ~2.7 carboxylic groups per molecule for the bulk SRFA. These values are in the range obtained also by *Ritchie and Perdue* [2003] for SRFA and *Tagliavini et al.* [2005] for HULIS extracted from smoke particles in Brazil.

3.3. Hygroscopic Growth

3.3.1. Hygroscopic Growth of SRFA Fractions

[22] Hydration and dehydration curves for the SRFA fractions and bulk are shown in Figure 3. Exponential-linear fit parameters for the hydration curves are given in Table 2. Hydration and dehydration did not show hysteresis (Figure 3). Neither deliquescence nor efflorescence were observed, consistent with results for standard humic substances tested by *Chan and Chan* [2003], *Brooks et al.* [2004], and *Svenningsson et al.* [2006]. *Gysel et al.* [2004] were the only ones to report hysteresis for aquatic Nordic References FA (NRFA). Figure 4 compares hydration curves for all the SRFA fractions and bulk. It can be seen that below RH of about 70%, the hydration curves for the fractions are nearly identical. The curves begin to diverge at higher values of RH. In the inset graph of Figure 4, it can be seen that in general, the smaller the molecular weight of the fraction, the greater the hygroscopic growth at high RHs.

[23] In the following we discuss hydration GF at 90% RH (GF_{90}), since below RH of 85%, particle growth is small (Figure 3) and measurements above 95% are not very accurate. Our results for SRFA GF_{90} (Figure 4 and Table 3) are similar to results reported earlier for other standard fulvic acids [*Chan and Chan*, 2003; *Brooks et al.*,

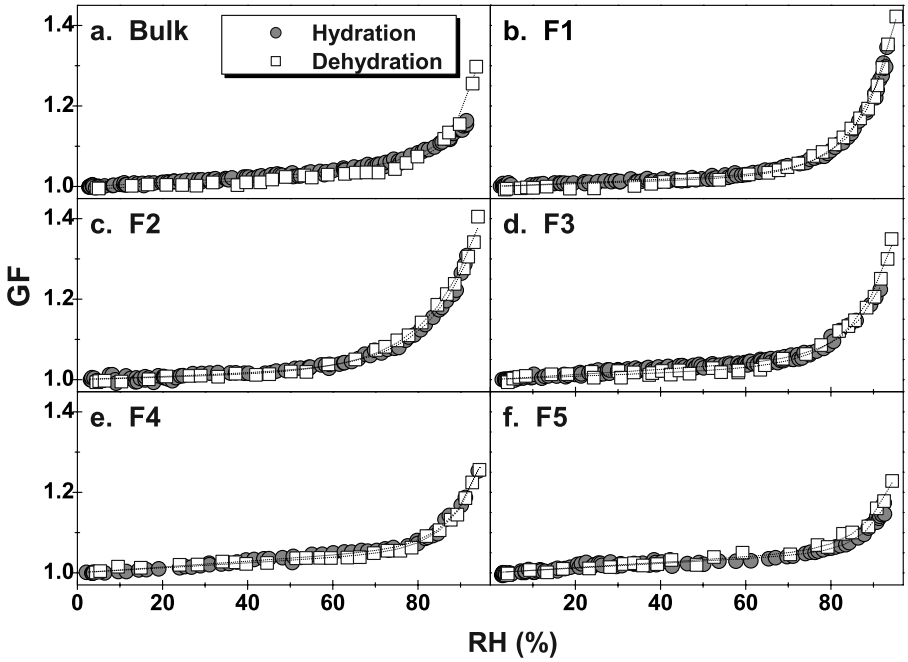

Figure 3. (a–f) Hydration and dehydration growth factors (GF) of Suwannee River fulvic acid (SRFA) samples. The open squares indicate the dehydration growth curve, while the gray circles show the hydration curve. The lines are exponential-linear fit with fit parameters shown in Table 2.

Table 2. Exponential-Linear Fit Parameters (y = p1*exp(−x/p2) + p3 + p4*x) p Values for Hydration Growth of all Samples

Sample	P1	P2	P3	P4	R^2
F1	2.310E-6	−7.964	1.000	4.3E-4	0.996
F2	5.000E-5	−10.720	1.000	3.8E-4	0.994
F3	2.027E-6	−8.071	1.000	6.3E-4	0.985
F4	1.329E-7	−6.647	1.000	7.2E-4	0.992
F5	1.197E-8	−5.780	1.000	5.9E-4	0.986
Bulk	3.000E-5	−11.280	1.000	5.2E-4	0.995
LBO-night	2.600E-4	−13.466	1.012	−4.0E-4	0.994
LBO-day	4.400E-4	−13.839	1.013	−7.7E-4	0.990
3WSFA	6.260E-3	−21.195	0.988	5.2E-4	0.997

2004; *Svenningsson et al.*, 2006]. Figure 5 shows the relationship between molecular weight, aromaticity, and acidity to GF_{90}. For the SRFA fractions, there is an inverse relationship between GF_{90} and molecular weight (Figure 5a) and GF_{90} and aromaticity (Figure 5b), and a direct relationship between GF_{90} and acidity (Figure 5c), with the exception of F1. An inverse relationship between GF_{90} and supersaturation CCN activation diameters [*Dinar et al.*, 2006] can also be seen in Figure 7, demonstrating that the more hygroscopic the material, the more CCN active it is. GF_{90} does not correlate well with either O/C ratio or with surface tension (ST_{90}), (Figures 5d and 5e). Using the exponential-linear fit we extrapolated the hydration curves up to RH = 95% (Figure 5f).

3.3.2. Hygroscopic Growth of HULIS Extracted From Atmospheric Particles

[24] Hydration and dehydration curves for the three HULIS samples are shown in Figures 6a–6c. As for SRFA, neither deliquescence nor efflorescence is observed. However, there is some hysteresis at RH < 60% and < 40% for LBO-night and LBO-day, respectively. Despite the preconditioning, a slight reduction in the GF (GF < 1) is observed at moderate RHs of ∼40–60% during hydration, probably owing to particle compaction following water uptake. Hysteresis and GF reduction were not observed in HULIS extracted from the air pollution particles, 3WSFA, or in conditioned SRFA. Such compaction phenomena was also reported by *Gysel et al.* [2004] for isolated organic matter from ambient continental-rural fine aerosol. *Gysel et al.* [2004] attributed this effect to restructuring influencing the mobility effective diameter obtained by the SMPS.

[25] Figure 6d superimposes the hydration curves for the three HULIS samples, the most hygroscopic SRFA fraction, F2, and the Bulk SRFA. Several observations are made: (1) HULIS isolated from the urban aerosol particles (3WSFA) are substantially more hygroscopic than HULIS extracted from the fresh and slightly aged biomass-burning samples (night and day, respectively); (2) the aged biomass-burning sample (LBO-day) is slightly more hygroscopic at RH > 90% than the fresh biomass-burning aerosol sample (LBO-night); (3) hygroscopic growth at 90% RH of both biomass-burning HULIS falls within the same range as for the small (F1 and F2) SRFA fractions; and (4) GF_{90} of urban aerosol-derived HULIS (3WSFA) is higher than that of even the most hygroscopic SRFA fractions (1.47 versus 1.23). The measured GF_{90} for the different samples are tabulated in Table 3. These results demonstrate that water uptake properties of HULIS vary as a function of its source (e.g., biomass burning or urban pollution) and the chemical and physical processes they undergo. The difference in hygroscopic growth between fresh and slightly aged biomass-burning HULIS (GF_{90} = 1.18 and 1.24, respectively) may be attributed to the smaller molecular weight of the aged biomass-burning HULIS. The aged biomass-burning extract is also less aromatic, further supporting the hypothesis that the daytime sample underwent some oxidation and may be more polar than the fresh sample.

[26] The relation between GF_{90} and the measured CCN activation diameter (D_{50}) [*Dinar et al.*, 2006] of the HULIS and the SRFA samples is shown in Figure 7. In this figure, SRFA samples are clearly distinguished from HULIS, appearing to represent two distinct populations. Within each population, an inverse relationship between GF_{90} and the critical particle activation diameter exists. One explanation of this unique distinction between HULIS and SRFA populations may be related to the greater surface activity of the HULIS samples as compared with the SRFA samples (Table 1). We also found that droplet activation of SRFA could be adequately modeled using a surface tension of water and a van't Hoff factor of 1.25, [*Dinar et al.*, 2006]. Since particles are relatively concentrated close to the CCN

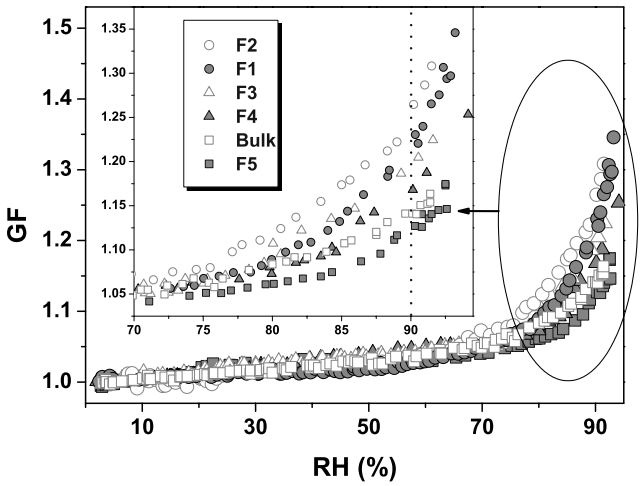

Figure 4. A superposition of hydration curves of SRFA samples. The GF_{90} values are presented in Table 3.

Table 3. Measured Cloud Condensation Nuclei Activation Diameters, D_{50}, as Measured by *Dinar et al.*, [2006] for Suwannee River Fulvic Acid, HULIS, and Ammonium Sulfate at SS-0.2%; Measured GF_{90} During Hydration; and Calculated GF_{95}[a]

Sample	SS-0.2%	GF_{90} (±0.008)[b]	GF_{95}[c]
F1	164.7 ± 14.8	1.23	1.39
F2	164.0 ± 14.3	1.25	1.39
F3	168.6 ± 10.6	1.20	1.32
F4	191.6 ± 12.1	1.17	1.28
F5	212.2 ± 11.8	1.12	1.22
Bulk	180.7 ± 13.4	1.13	1.18
LBO-night	133.8 ± 11.1	1.18	1.27
LBO-day	99.4 ± 7.4	1.24	1.36
3WSFA	81.0 ± 5.6	1.47	1.59
Ammonium sulfate	79.8 ± 6.9	1.67	1.97

[a]GF standard deviation values do not exceed a GF of ±0.008, which corresponds to a change in the monodisperse spectra mean diameter of ∼±0.5 nm (for GF_{90} = ∼1.23).
[b]Values are measured.
[c]Values are extrapolated.

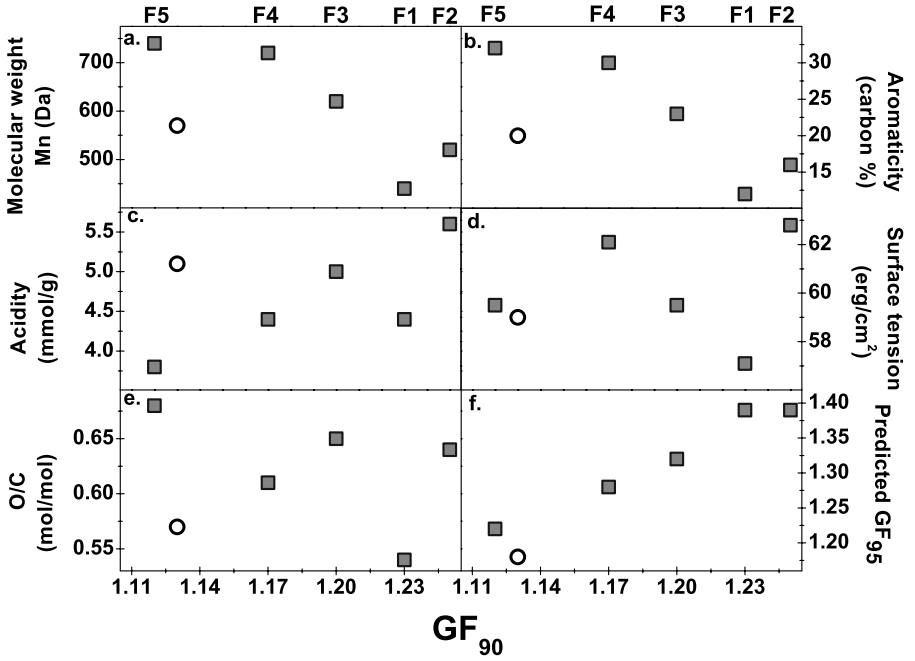

Figure 5. Correlations of various chemical parameters with GF_{90} for SRFA samples. (a) UV-correlated molecular weight (M_N). (b) UV-correlated aromaticity content. (c) Measured acidity. (d) Surface tension. (e) O/C molar ratio. (f) Fit extrapolation to GF_{95}. The gray squares represent the fractions samples as marked at the top of the figure, while the open circles indicate the results for the bulk sample.

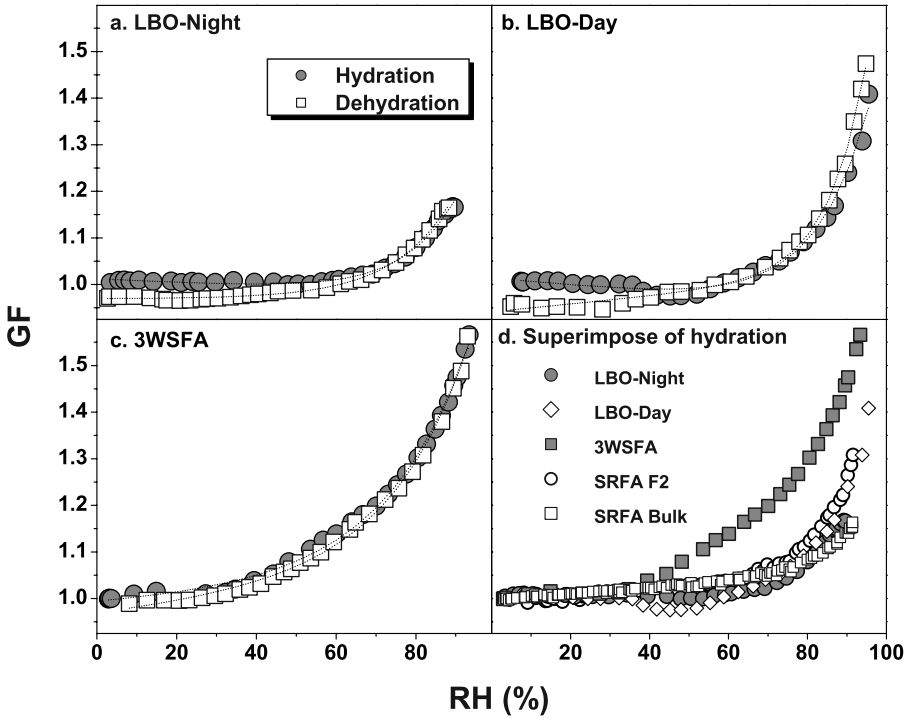

Figure 6. Hydration and dehydration growth factors (GF) as a function of % RH for humic-like substances (HULIS) samples. The open squares indicate the dehydration growth curve, and the gray circles show the hydration growth curve. (a) Lag B'Omer (LBO)–night, from fresh smoke particles. (b) LBO-day, from slightly aged smoke particles. (c) 3WSFA, from daytime photochemical pollution particles. The lines represent the exponential-linear fit with fit parameters shown in Table 2. (d) Superposition of the hydration curves of the three HULIS samples, the most hygroscopic SRFA sample, F2, and SRFA bulk sample.

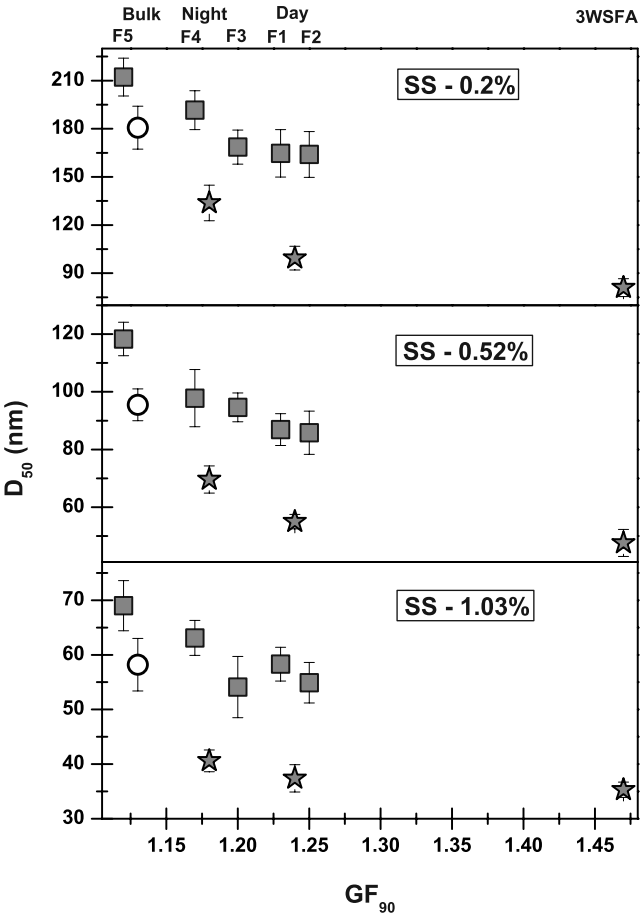

Figure 7. HULIS and all SRFA samples (fractions and bulk) GF_{90} versus critical diameter of activation (D_{50}) for SS: (top) 0.2%, (middle) 0.52%, and (bottom) 1.03. The data for SS-0.2% are presented in Table 3. The gray squares represent the SRFA fractions as marked at the top of the figure, the SRFA Bulk sample is represented by open circles, and the HULIS samples are shown by gray stars. The different fractions and samples are denoted at the top.

activation, the extent of dissociation is expected to be less than 25%, and therefore the 1.25 factor should be viewed as a summed measure of the degree of dissociation, nonideal behavior, and uncertainties in the determination of molecular weight. Previously, we found that SRFA activation data could be reasonably modeled to better than 10% by using water surface tension and a van't Hoff factor of 1.25 [*Dinar et al.*, 2006]. Yet, in contrast to SRFA, the activation of atmospheric HULIS could not be reasonably modeled using a surface tension of water, because it required unrealistic estimates of van't Hoff factors (*i* of 4.5 for LBOs and 9 for 3WSFA). Therefore it was concluded that surface tension is an important parameter for modeling CCN activation of HULIS. If surface tension (and its dynamic properties, i.e., how long it takes to reach equilibrium surface tension) is not known, it may then be difficult to estimate particle activation on the basis of hygroscopic growth curves. It also can be noted that surface tension at the time of activation may be substantially different compared with the equilibrium surface tension for 1 g L^{-1} solutions reported here, given kinetics of dissolution, diffusion, and adsorption of surface active compounds at the surface of the growing drop. The possibility of predicting particle activation from hygroscopic growth curves is explored in the next section.

3.4. CCN Activation Modeling Approach Based on the Hygroscopic Growth Factors

[27] Recently, Kreidenweis and coworkers [*Brechtel and Kreidenweis*, 2000a, 2000b; *Koehler et al.*, 2006; *Kreidenweis et al.*, 2005] developed a framework for estimating CCN activity from subsaturation hygroscopic growth behavior. In this section, we employ this approach, using the hygroscopic growth data presented herein, to predict CCN activation diameters measured by *Dinar et al.* [2006] for the same materials.

[28] The equilibrium saturation ratio of water above an aqueous solution droplet (diameter D_{wet}), S_{wat}, is given by the following relation [*Kreidenweis et al.*, 2005; *Seinfeld and Pandis*, 1998]:

$$S_{wat} = a_w(x) \times Ke,$$
$$Ke = \exp\left(\frac{4MW_w\sigma_{sol}}{RT\rho_w D_{wet}}\right). \quad (1)$$

[29] Here $a_w(x)$ is the water activity, x is the solute mole fraction, Ke is the Kelvin term that accounts for the effect of the droplet curvature, MW_w is the molecular weight of water, σ_{sol} is the droplet surface tension, R is the gas constant, T is the temperature, and ρ_w is the water density. Provided that the Kelvin term and the water activities for a sufficiently wide range of mole fractions are known, S_{wat} can be calculated as a function of D_{wet}, the diameter of the wet particle. The calculation yields a Köhler curve with a maximum at the droplet critical supersaturation, that is, a supersaturation needed for activation and growth to a cloud droplet. For most atmospheric organic species, including those studied here, the required activity data is not available. Therefore we extract the needed activity data from the H-TDMA measurements using the method presented by *Kreidenweis et al.* [2005], which is based on fitting the measured growth factors to the following function of the activity, a_W:

$$GF = \left[1 + \left(a + b \times a_w + c \times a_w^2\right)\frac{a_w}{1 - a_w}\right]^{1/3}, \quad (2)$$

where *a, b,* and *c* are the fitting parameters. We neglect the Kelvin effect, which allows for equating the activities in equation (2) with RHs applied in the H-TDMA experiments. This can be considered as a valid approximation, since associated errors are 5% at maximum at the diameter range above 50 nm. Moreover, we present results based on the fits of the hydration part of the hydration/dehydration cycle of the samples, since the particles did not undergo deliquescence prior to their entrance into the CCN chamber.

[30] In order to compare the predicted activation behavior with the experimental results, we calculated the dry activa-

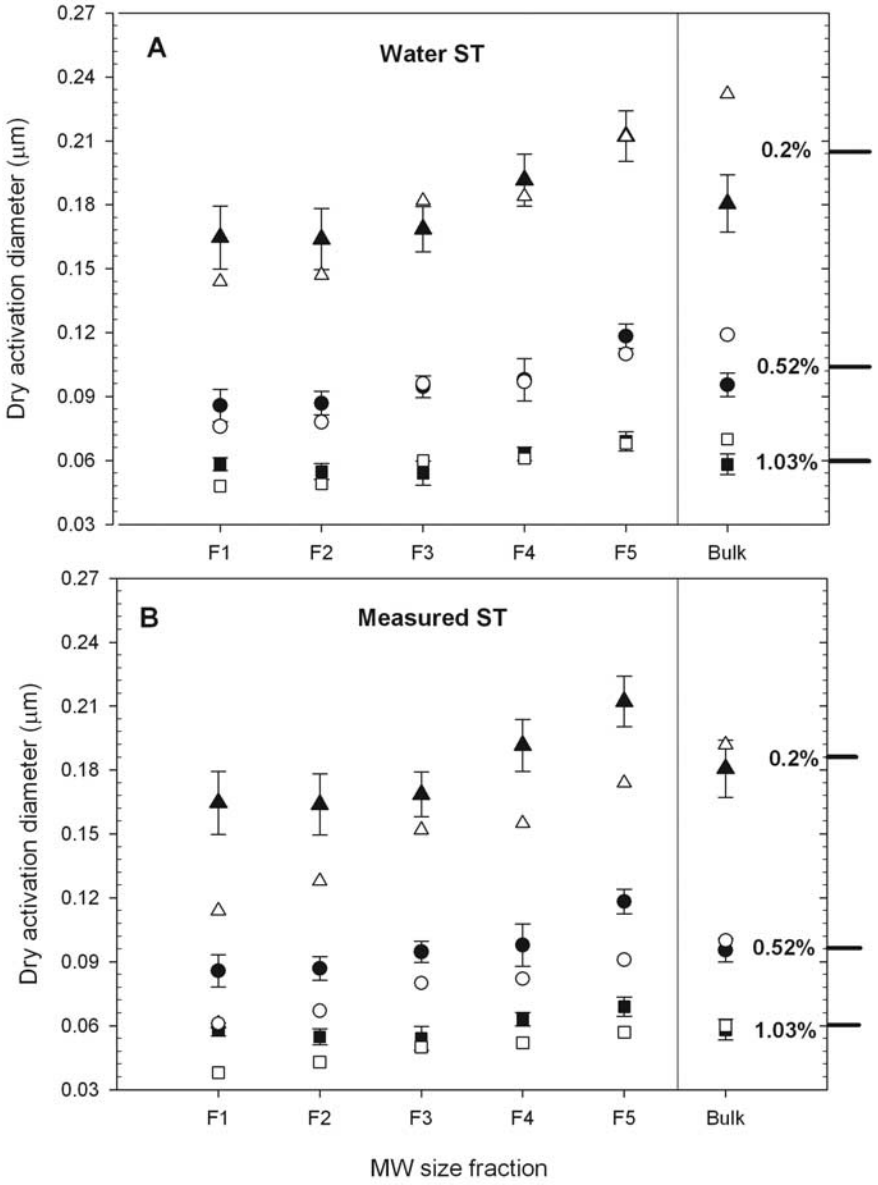

Figure 8. Measured (solid symbols) and predicted (open symbols) dry diameters needed for particle activation for SRFA. Squares, circles, and triangles indicate the activation diameters at supersaturations 0.2, 0.52, and 1.03%, respectively. The particle surface tension, σ_{sol}, is (a) set equal to that of water and (b) taken from the measurements.

tion diameters, D_{calc}, which is the dry diameter needed for activation at a certain water SS. They are obtained by calculating Köhler curves using equation (1) and searching for dry diameters for which the critical SS correspond to the SS used in the experiments. The water activity $a_w(x)$ in equation (1) was calculated as described by *Kreidenweis et al.* [2005], and the Kelvin term *Ke* was calculated using two different values for the surface tension (σ_{sol}): that of water and that measured at the concentration of 1 g/L. This was done in order to investigate whether the studied substances influence CCN activation by decreasing the surface tension. Finally, it should be noted that the method is insensitive to the particle dry density as long as the same value is applied throughout the procedure [*Kreidenweis et al.*, 2005].

3.4.1. Predicted Activation Diameters for the SRFA Samples

[31] A comparison of the predicted (by the method by *Kreidenweis et al.* [2005] and *Koehler et al.* [2006]) and measured [*Dinar et al.*, 2006] dry activation diameters for the SRFA samples is shown in Figure 8. A good agreement was reached when σ_{sol} was assumed to be that of water, D_{calc} being generally within the experimental uncertainties (Figure 8a), except for the bulk samples. When the measured surface tensions are used in equation (1), values of D_{calc} decrease by 14–28% (Figure 8b). Excluding the bulk samples, this underpredicts D_{50}, supporting the notion that SRFA did not affect CCN activation by reducing the particle surface tension notably [*Dinar et al.*, 2006]. The difference

in the predictions between the bulk and molecular weight-fractionated samples is probably due to the lack of hygroscopic growth data for RHs above 92% for the bulk samples, which causes large uncertainties to the predicted water activity as the method is based on extrapolating the measured hygroscopic growth behavior to larger water vapor saturation levels.

[32] In our previous study [*Dinar et al.*, 2006], we calculated the dry activation diameters for the SRFA samples using an approximate expression for the activity term in the Köhler equation together with information on the sample molecular weights and surface tensions. These predictions display a good agreement with the CCN data when the van't Hoff factor which accounts for a nonideal behavior of the droplets was set to 1.25, or alternatively, the surface tension was decreased by 15–25%. Evoking the van't Hoff factor is consistent with the estimates of dissociation extent. Therefore both the present results and those of *Dinar et al.* [2006] suggest that SRFA surface tension lowering properties do not influence particle activation. This may be a result of diffusion, dissolution, or adsorption limitations.

[33] It is noted, though, that the calculations are based on an assumption of one narrow number average molecular weight which was estimated from UV correlations. In reality (in both CCN and HG experiments) the bulk SRFA sample contains a broader distribution of molecular weights, while the fractions have a much narrower distribution and hence the assumed molecular weight presents better the reality. This may lead to substantially higher errors in the modeling of bulk as compared to the fractions.

3.4.2. Predicted Activation Diameters for the Extracted HULIS Samples

[34] The same procedure was repeated for the HULIS samples extracted from ambient aerosols and the results are displayed in Figure 9. D_{50} are consistently overpredicted when the particle ST is assumed to be that of water (Figure 9a), the discrepancies being largest for the LBO-night samples. The agreement improves when the measured surface tensions are applied, D_{calc} being within the measurement error limits for the LBO-day samples. D_{50} are still slightly overpredicted for the other two samples at the lower super saturations (Figure 9b). Furthermore, the D_{calc} values for the LBO-day and 3WSFA samples are very close to each other, although D_{50} were clearly smaller for the 3WSFA samples. This is explained by the somewhat lower ST of the 3WSFA HULIS (Table 1). In fact, additional sensitivity calculations show that a good agreement with the data is obtained by assuming a lower ST than what was measured, that is, around 45 mN/m (not shown in the figure). With respect to the LBO-night sample, the sensitivity analysis showed that the results are consistent with ST around 38 mN/m (not illustrated by a figure). The role of the ST remains somewhat unclear in this case, however, since the hygroscopic growth measurements extend only up to ~93% RH, which causes larger uncertainties to the fit used for predicting the water activity in equation (1). To summarize, the results for the LBO-day and 3WSFA sample suggest that HULIS present in ambient particles may affect CCN activation through reducing the particle surface tension. The conclusion is also in agreement with our previous study. However, the strong sensitivity of the fit to the hygroscopic growth behavior at very high RH, and the steep increase in the GF at these relative humidity levels limits to some extent the ability to accurately predict the activation diameters of such species. It could be argued that some of the discrepancy between observed dry activation diameters and the model results obtained using the measured surface tension be explained by uncertainties in the water activity. However, a set of sensitivity studies (not shown) was conducted. The results show that the uncertainties due to the water activities are small and that they cannot explain the discussed discrepancy.

3.5. General Aspects: Symptomatic Behavior as Diagnostics of HULIS

[35] Organic compounds of relatively high molecular weight that are difficult to speciate are abundant in atmospheric aerosols. One way to approach the problem of speciation is by classifying the compounds into broad chemical classes on the basis of general chemical indicators (such as elemental composition, mean molecular weight, acidity, functional group composition, etc.). A complementary approach would be to test the physical behavior of the substances of interest (for example, surface tension and hygroscopicity). These two approaches, combined in this study, have rendered some important insights into atmospheric HULIS as compared with a model HULIS (Suwannee River fulvic acid).

[36] In this work and in that of *Dinar et al.* [2006], we demonstrated that measuring the interaction of particles with water vapor, thereby probing a set of physicochemical properties (parameters in Raoult and Kelvin terms of the Köhler equation), is useful in two ways. First, it delivers growth factors and critical radii of activation that are needed for understanding the climatic and environmental effects of aerosols that are dominated by such species. At the same time, it serves as an additional means of classifying compounds that are not easily chemically speciated.

[37] In a comparison of estimated mean molecular weights with aromaticity (Table 1), HULIS derived from fresh wood-burning aerosol (LBO-night) resemble the F3 fraction of SRFA, while HULIS derived from aged wood-burning aerosol (LBO-day) is more similar to SRFA fractions F1 and F2. The urban pollution-derived HULIS sample (3WSFA) is similar to fraction F2. For both fresh and aged wood-burning aerosol-derived HULIS, the resemblance to the respective SRFA holds also for subsaturation growth factors at 90% and 95% relative humidity (GF_{90} and GF_{95}) (Table 3). However, the growth factors of the 3WSFA HULIS sample are 15%–20% larger than any of the SRFA fractions (or bulk). Considering CCN activation (Table 3), all atmospheric samples are considerably more CCN-active than the SRFA fractions and bulk, which might be attributed to the distinctively lower surface tension of the atmospheric samples.

[38] Our results indicate that HULIS derived from fresh wood-burning particles are relatively more similar to SRFA with regards to hygroscopic growth and to some extent, CCN activity, while the aged smoke-derived HULIS are less similar. The urban pollution-derived HULIS sample (3WSFA) has different hygroscopic growth and activation behavior altogether than SRFA. The increasing dissimilarities between HULIS and SRFA with increasing residence time in the atmosphere may be attributed to mixing with different organic species that are operationally extractable

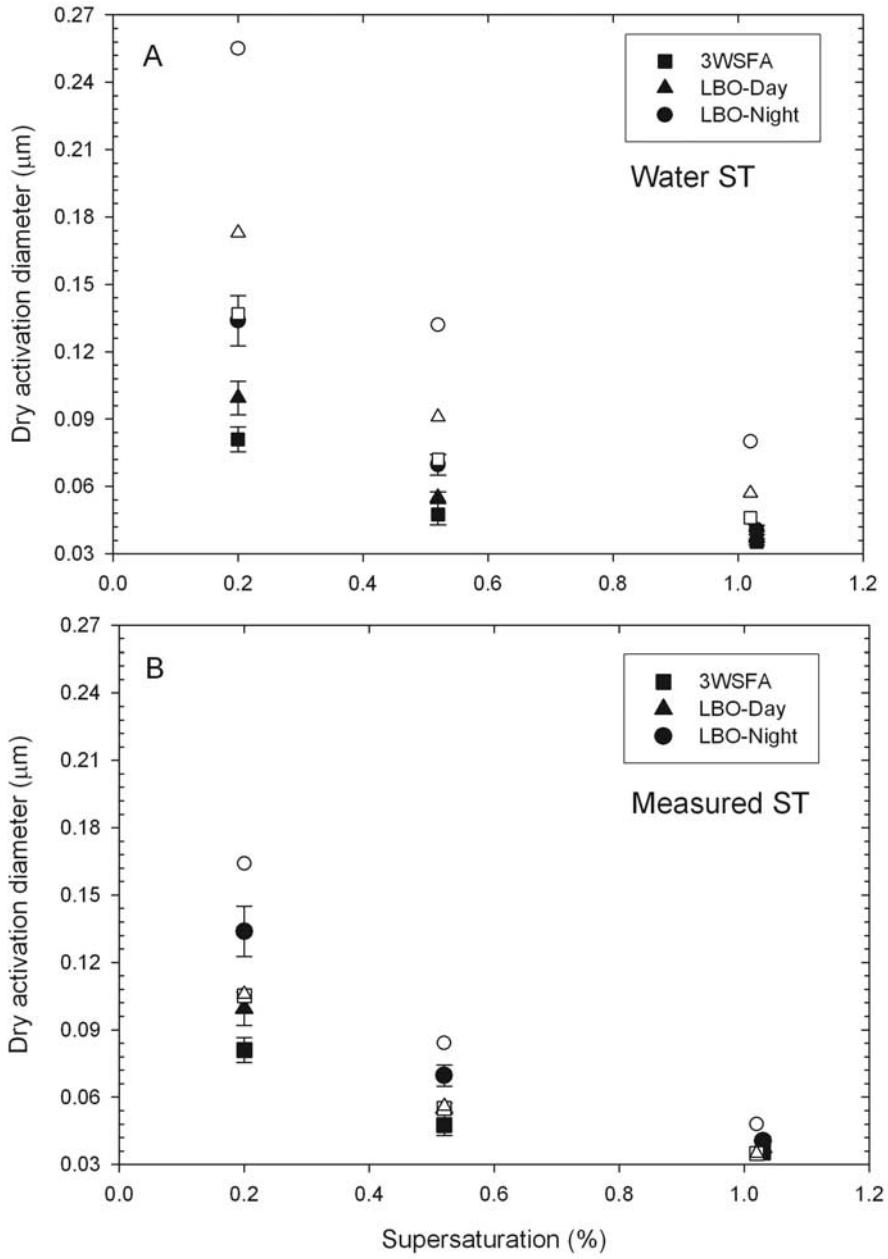

Figure 9. Measured (solid symbols) and predicted (open symbols) dry diameters needed for particle activation of the HULIS samples extracted from ambient aerosols. The particle surface tension, σ_{sol}, (a) set equal to that of water and (b) taken from the measurements.

as FA, but have different properties (although it was verified that the samples do not contain inorganic ions or low molecular weight organic acids). Alternatively, the effect of residence time on the disparity between HULIS and SRFA may be attributed to chemical processing in the atmosphere. For example, the fresh wood-burning HULIS (LBO-night) can be reasonably considered to contain more cellulose-like and lignin-like moieties that confer on HULIS certain similarities to fulvic acid. These moieties then undergo some degree of degradation via photooxidative processes, as represented by the aged biomass-burning HULIS (LBO-day). Molecular structures derived from such photooxidative processes may have different water vapor interaction attributes than those derived from the microbial-mediated oxidative processes which are responsible for fulvic acid formation in soils and aquatic environments. Hence atmospheric HULIS are not necessarily similar to model fulvic acids, as clearly illustrated by the results presented herein. As such, general conclusions for atmospheric HULIS drawn from model soil and aquatic humic substances should be made with extra care [*Graber and Rudich*, 2006].

4. Summary

[39] Hygroscopic growth at subsaturation conditions of molecular weight-fractionated and bulk Suwannee River fulvic acid and of HULIS extracted from ambient aerosols

were measured in a humidity tandem DMA set up. The results show that the hygroscopic growth of particles composed of these species has no deliquescence or efflorescence. For molecular weight-fractionated SRFA samples, the growth factor at ~90% RH is molecular weight dependent with the smallest growth factor for the highest molecular weight fraction, as expected from Raoult's law. The aerosol HULIS extracts exhibit hygroscopic growth behavior that depends on source and atmospheric residence time. The results suggest that the SRFA and aerosol-derived HULIS from aerosols may represent different species with somewhat different hygroscopic and activation behavior.

[40] We attempted to use the model presented by *Kreidenweis et al.* [2005] to predict CCN activation of these aerosols on the basis of their hygroscopic growth curves. It is shown that this approach can be used reasonably well for SRFA fractions, but is limited in use for the HULIS extracted from aerosol particles. This may result from several reasons:

[41] 1. Surface tension does not seem to play a role in the CCN activation of SRFA; hence predictions from subsaturation conditions are more straightforward.

[42] 2. Surface tension may play a role in the activation of HULIS.

[43] 3. Owing to the small growth at low RH and higher growth at high RH, the method presented by *Kreidenweis et al.* [2005] is very sensitive to the behavior of the sample at the highest RH. For experimental reasons, results from this RH region have higher uncertainty and hence the prediction to supersaturation conditions is more difficult and bears substantially more error.

[44] Despite these difficulties, the *Kreidenweis et al.* [2005] method is useful even for these organic species and may be used as good estimate for CCN activity when direct CCN measurements are not available.

[45] **Acknowledgments.** We thank two anonymous referees for their thoughtful remarks. Stimulating discussions with Doug Worsnop (Aerodyne Research Inc.) are highly appreciated. T. A. acknowledges financial support from the Helsingin Sanomat Centennial Foundation. Valuable help from Doron Lahav (Ashdod-Hevel Yavne Regional Association for Environmental Protection) is acknowledged. Aerosol ambient concentrations were provided by the Israel Ministry of Environment. This work was supported by research grants from the Israeli Academy of Sciences (grant 162/05) and the Minerva Foundation.

References

Abdul-Razzak, H., and S. J. Ghan (2004), Parameterization of the influence of organic surfactants on aerosol activation, *J. Geophys. Res.*, *109*, D03205, doi:10.1029/2003JD004043.

Andreae, M. O., et al. (2005), Strong present-day aerosol cooling implies a hot future, *Nature*, *435*, 1187–1190.

Bragatto, P., et al. (2002), Measurement of airborne particles number and size in ambient air quality assessment, *Fresenius Environ. Bull.*, *11*, 182–185.

Brechtel, F. J., and S. M. Kreidenweis (2000a), Predicting particle critical supersaturation from hygroscopic growth measurements in the humidified TDMA. part I: Theory and sensitivity studies, *J. Atmos. Sci.*, *57*, 1854–1871.

Brechtel, F. J., and S. M. Kreidenweis (2000b), Predicting particle critical supersaturation from hygroscopic growth measurements in the humidified TDMA. part II: Laboratory and ambient studies, *J. Atmos. Sci.*, *57*, 1872–1887.

Brooks, S. D., et al. (2004), Water uptake by particles containing humic materials and mixtures of humic materials with ammonium sulfate, *Atmos. Environ.*, *38*, 1859–1868.

Cappiello, A., et al. (2003), Molecular characterization of the water-soluble organic compounds in fog water by ESIMS/MS, *Environ. Sci. Tech.*, *37*, 1229–1240.

Chan, M. N., and C. K. Chan (2003), Hygroscopic properties of two model humic-like substances and their mixtures with inorganics of atmospheric importance, *Environ. Sci. Tech.*, *37*, 5109–5115.

Chan, M. N., and C. K. Chan (2005), Mass transfer effects in hygroscopic measurements of aerosol particles, *Atmos. Chem. Phys.*, *5*, 4057–4082.

Chin, Y. P., et al. (1994), Molecular-weight, polydispersity, and spectroscopic properties of aquatic humic substances, *Environ. Sci. Tech.*, *28*, 1853–1858.

Cini, R., et al. (1996), Air-sea exchange: Sea salt and organic micro components in Antarctic snow, *Int. J. Environ. Anal. Chem.*, *63*, 15–27.

Cruz, C. N., and S. N. Pandis (2000), Deliquescence and hygroscopic growth of mixed inorganic-organic atmospheric aerosol, *Environ. Sci. Tech.*, *34*, 4313–4319.

Cziczo, D. J., and J. P. D. Abbatt (1999), Deliquescence, efflorescence, and supercooling of ammonium sulfate aerosols at low temperature: Implications for cirrus cloud formation and aerosol phase in the atmosphere, *J. Geophys. Res.*, *104*, 13,781–13,790.

Decesari, S., et al. (2000), Characterization of water-soluble organic compounds in atmospheric aerosol: A new approach, *J. Geophys. Res.*, *105*, 1481–1490.

Decesari, S., et al. (2001), Chemical features and seasonal variation of fine aerosol water-soluble organic compounds in the Po Valley, Italy, *Atmos. Environ.*, *35*, 3691–3699.

Dinar, E., et al. (2006), Cloud condensation nuclei properties of model and atmospheric HULIS, *Atmos. Chem. Phys.*, *6*, 2465–2481.

Eastoe, J., and J. S. Dalton (2000), Dynamic surface tension and adsorption mechanisms of surfactants at the air-water interface, *Adv. Colloid Interface Sci.*, *85*, 103–144.

Facchini, M. C., et al. (1999a), Partitioning of the organic aerosol component between fog droplets and interstitial air, *J. Geophys. Res.*, *104*, 26,821–26,832.

Facchini, M. C., et al. (1999b), Cloud albedo enhancement by surface-active organic solutes in growing droplets, *Nature*, *401*, 257–259.

Facchini, M. C., et al. (2000), Surface tension of atmospheric wet aerosol and cloud/fog droplets in relation to their organic carbon content and chemical composition, *Atmos. Environ.*, *34*, 4853–4857.

Fuzzi, S., et al. (2001), A simplified model of the water soluble organic component of atmospheric aerosols, *Geophys. Res. Lett.*, *28*, 4079–4082.

Graber, E. R., and Y. Rudich (2006), Atmospheric HULIS: How humic-like are they? A comprehensive and critical review, *Atmos. Chem. Phys.*, *6*, 729–753.

Gysel, M., et al. (2002), Hygroscopicity of aerosol particles at low temperatures. 2. Theoretical and experimental hygroscopic properties of laboratory generated aerosols, *Environ. Sci. Tech.*, *36*, 63–68.

Gysel, M., et al. (2004), Hygroscopic properties of water-soluble matter and humic-like organics in atmospheric fine aerosol, *Atmos. Chem. Phys.*, *4*, 35–50.

Haiber, S., et al. (2001), Two-dimensional NMR studies of size fractionated Suwannee River fulvic and humic acid reference, *Environ. Sci. Tech.*, *35*, 4289–4294.

Hansen, J., et al. (2005), Efficacy of climate forcings, *J. Geophys. Res.*, *110*, D18104, doi:10.1029/2005JD005776.

Havers, N., et al. (1998), Spectroscopic characterization of humic-like substances in airborne particulate matter, *J. Atmos. Chem.*, *29*, 45–54.

Herckes, P., et al. (2002), Organic matter in Central California radiation fogs, *Environ. Sci. Tech.*, *36*, 4777–4782.

Intergovernmenta Panel on Climate Change (1995), *Intergovernmental Panel on Climate Change*, Cambridge Univ. Press, New York.

Intergovernmental Panel on Climate Change (2001), *Climate Change: The Scientific Basis*, Cambridge Univ. Press, New York.

Kaufman, Y. J., et al. (2005), The effect of smoke, dust, and pollution aerosol on shallow cloud development over the Atlantic Ocean, *Proc. Natl. Acad. Sci. U. S. A.*, *102*, 11,207–11,212.

Kiss, G., et al. (2002), Characterization of water-soluble organic matter isolated from atmospheric fine aerosol, *J. Geophys. Res.*, *107*(D21), 8339, doi:10.1029/2001JD000603.

Kiss, G., et al. (2003), Estimation of the average molecular weight of humic-like substances isolated from fine atmospheric aerosol, *Atmos. Environ.*, *37*, 3783–3794.

Kiss, G., et al. (2005), Surface tension effects of humic-like substances in the aqueous extract of tropospheric fine aerosol, *J. Atmos. Chem.*, *50*, 279–294.

Koehler, K. A., et al. (2006), Water activity and activation diameters from hygroscopicity data - part II: Application to organic species, *Atmos. Chem. Phys.*, *6*, 795–809.

Koren, I., et al. (2005), Aerosol invigoration and restructuring of Atlantic convective clouds, *Geophys. Res. Lett.*, *32*, L14828, doi:10.1029/2005GL023187.

Kramer, L., et al. (2000), Microstructural rearrangement of sodium chloride condensation aerosol particles on interaction with water vapor, *J. Aerosol Sci.*, *31*, 673–685.

Kreidenweis, S. M., et al. (2005), Water activity and activation diameters from hygroscopicity data - part I: Theory and application to inorganic salts, *Atmos. Chem. Phys.*, *5*, 1357–1370.

Krivacsy, Z., et al. (2000), Study of humic-like substances in fog and interstitial aerosol by size-exclusion chromatography and capillary electrophoresis, *Atmos. Environ.*, *34*, 4273–4281.

Krivacsy, Z., et al. (2001), Study on the chemical character of water soluble organic compounds in fine atmospheric aerosol at the Jungfraujoch, *J. Atmos. Chem.*, *39*, 235–259.

Mayol-Bracero, O. L., et al. (2002), Water-soluble organic compounds in biomass burning aerosols over Amazonia: 2. Apportionment of the chemical composition and importance of the polyacidic fraction, *J. Geophys. Res.*, *107*(D20), 8091, doi:10.1029/2001JD000522.

Menache, M. G., et al. (1996), An empirical dosimetry model of aerodynamic particle deposition in the rat respiratory tract, *Inhal. Toxicol.*, *8*, 539–578.

Mikhailov, E., et al. (2004), Interaction of aerosol particles composed of protein and salts with water vapor: Hygroscopic growth and microstructural rearrangement, *Atmos. Chem. Phys.*, *4*, 323–350.

Mircea, M., et al. (2002), The influence of the organic aerosol component on CCN supersaturation spectra for different aerosol types, *Tellus, Ser. B*, *54*, 74–81.

Nenes, A., et al. (2002), Can chemical effects on cloud droplet number rival the first indirect effect?, *Geophys. Res. Lett.*, *29*(17), 1848, doi:10.1029/2002GL015295.

Novakov, T., and C. E. Corrigan (1996), Cloud condensation nucleus activity of the organic component of biomass smoke particles, *Geophys. Res. Lett.*, *23*, 2141–2144.

Peuravuori, J., and K. Pihlaja (1997), Molecular size distribution and spectroscopic properties of aquatic humic substances, *Anal. Chim. Acta*, *337*, 133–149.

Raes, F., et al. (2000), Formation and cycling of aerosols in the global troposphere, *Atmos. Environ.*, *34*, 4215–4240.

Ramachandran, G., et al. (1996), Assessment of particle size distributions in workers' aerosol exposures, *Analyst*, *121*, 1225–1232.

Ramanathan, V., et al. (2001), Atmosphere, aerosols, climate, and the hydrological cycle, *Science*, *294*, 2119–2124.

Ritchie, J. D., and E. M. Perdue (2003), Proton-binding study of standard and reference fulvic acids, humic acids, and natural organic matter, *Geochim. Cosmochim. Acta*, *67*, 85–96.

Rosenfeld, D. (2000), Suppression of rain and snow by urban and industrial air pollution, *Science*, *287*, 1793–1796.

Rostad, C. E., and J. A. Leenheer (2004), Factors that affect molecular weight distribution of Suwannee river fulvic acid as determined by electrospray ionization/mass spectrometry, *Anal. Chim. Acta*, *523*, 269–278.

Samburova, V., et al. (2005), Characterization of high molecular weight compounds in urban atmospheric particles, *Atmos. Chem. Phys.*, *5*, 2163–2170.

Saxena, P., and L. M. Hildemann (1996), Water-soluble organics in atmospheric particles: A critical review of the literature and application of thermodynamics to identify candidate compounds, *J. Atmos. Chem.*, *24*, 57–109.

Schafer, A. I., et al. (2002), Charge effects in the fractionation of natural organics using ultrafiltration, *Environ. Sci. Tech.*, *36*, 2572–2580.

Seinfeld, J. H., and S. N. Pandis (1998), *Atmospheric Chemistry and Physics: From Air Pollution to Climate Change*, John Wiley, New York.

Simoneit, B. R. (1980), Eolian particulates from oceanic and rural areas: Their lipids, fulvic and humic acids and residual carbon, *Phys. Chem. Earth*, *12*, 343–352.

Svenningsson, B., et al. (2006), Hygroscopic growth and critical supersaturations for mixed aerosol particles of inorganic and organic compounds of atmospheric relevance, *Atmos. Chem. Phys.*, *6*, 1937–1952.

Tagliavini, E., et al. (2005), Functional group analysis by H NMR/chemical derivatization for the characterization of organic aerosol from the SMOCC field campaign, *Atmos. Chem. Phys. Disc.*, *5*, 9447–9491.

Varga, B., et al. (2001), Isolation of water-soluble organic matter from atmospheric aerosol, *Talanta*, *55*, 561–572.

Virtanen, A. K. K., et al. (2004), Effect of engine load on diesel soot particles, *Environ. Sci. Tech.*, *38*, 2551–2556.

Weingartner, E., et al. (1995), Growth and structural-change of combustion aerosols at high relative-humidity, *Environ. Sci. Tech.*, *29*, 2982–2986.

Zappoli, S., et al. (1999), Inorganic, organic and macromolecular components of fine aerosol in different areas of Europe in relation to their water solubility, *Atmos. Environ.*, *33*, 2733–2743.

T. Anttila, Research and Development, Finnish Meteorological Institute, 00101 Helsinki, Finland.

E. Dinar, Y. Rudich, and I. Taraniuk, Department of Environmental Sciences, Weizmann Institute of Science, Rehovot 76100, Israel. (yinon@wisemail.weizmann.ac.il)

E. R. Graber, Institute of Soil, Water, and Environmental Sciences, Volcani Center, A.R.O., Bet Dagan 50250, Israel.

T. F. Mentel, Institute for Tropospheric Chemistry, Research Center Jülich, 52425 Jülich, Germany.